IJMOT

INTERNATIONAL JOURNAL OF MICROWAVE AND OPTICAL TECHNOLOGY,

VOL.8, NO.3, MAY 2013

A Sampling Oscilloscope Based System with Active RF/IF Load-pull for Multi-Tone Non-linear Device Characterization

[1]Muhammad Akmal Chaudhary, [2]Jonathan Lees, [2]Johannes Benedikt, [2]Paul Tasker

[1]Department of Electrical Engineering, Ajman University of Science & Technology, Ajman, UAE
[2]Center for High Frequency Engineering, Cardiff University, Wales, CF24 3AA, U.K.
Tel: 971-6705-6892; E-mail: m.akmal@ajman.ac.ae

***Abstract*- This paper presents a fully automated measurement system based around a Tektronix sampling oscilloscope. The system is capable of measuring calibrated time domain voltage and current waveforms at the device plane. A novel active load-pull loop is incorporated which has proved very useful for increasing the speed of multi-tone device characterization, moreover the architecture opens up the possibility of multi-tone load pull measurements, novel concepts are discussed which explain how the system can be used to perform non-linear device characterization in real time, the system also incorporates an intermediate frequency (IF) test set to measure the complete waveforms, which could be useful in characterization of memory effects. Triggering issues of sampling oscilloscopes are discussed in some detail along with a novel sampling approach which allows for more efficient measurement of multi-tone waveforms. Some interesting applications of the system are also introduced.**

***Index Terms*- Baseband, Gallium Nitride (GaN), linearity, load-pull, multi-tone, power transistor.**

I. INTRODUCTION

The generic multi-tone waveform measurement system architecture is shown in figure 1, as the Tektronix sampling oscilloscope is 4 channel receiver, the architecture is simpler than that shown in [1-3], upon which this measurement architecture is based. The system uses two broad-band directional couplers to simultaneously measure all four incident (a) and reflected (b) waves. DC biasing of the device is achieved using bias-tees, as the DC signals can not be measured through the couplers, a computer controlled DC source is used, and the full waveforms are then produced by inserting the DC voltage and current information into the measured RF waveform. At this point the measurement system was compared to a system currently in use at the university; the measured waveforms compared very well to those measured using a system based around Agilent microwave transition analyzer (MTA). It is important to note that the MTA based system had recently successfully been compared to other large signal network analyzers (LSNA's) throughout Europe, through research completed by TARGET (Top Amplifier Research Groups in a European Team).

As the system was to be used to characterize non-linear devices obviously some load-pull capabilities were required. Traditionally load-pull, emulation of load impedance, has been achieved using passive techniques [4-5], however, limitations are introduced due to losses in the network between the device under test (DUT) and the tuner, which reduce the maximum reflection coefficient obtainable. The solution to this problem is active load-pull where emulation of load impedance is achieved by injecting an amplified signal of specific magnitude and phase into the DUT output. Such active systems can have either an "open loop" or "closed loop" architecture.

In a "closed loop" system, first presented in [6], the injected signal is a modified version (direct function) of the DUT output signal. This ensures that the emulated load impedance (matching circuit) is independent of drive level; however this architecture is prone to oscillations. In the alternative "open loop" system, first introduced

in [7], the injected signal is generated independently. This avoids the oscillation problem but now, to maintain a constant emulated load impedance (reflection coefficient) under changing drive conditions, results in a slow iterative process; a number of magnitude and phase adjustments, manual or automated, of the injected signal are needed to maintain the target reflection coefficient, the current MTA system is set up in this way and has proved prohibitive to certain measurements, most importantly it should be mentioned that such systems are unsuitable for multi-tone measurements as the number of signal sources required makes the measurement set-up far too expensive and physically impractical.

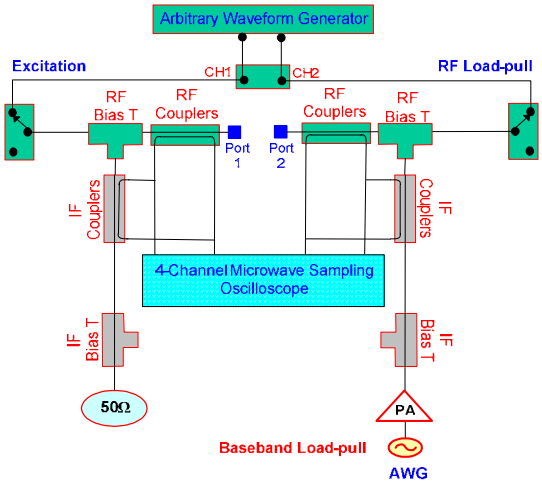

Fig. 1. Refined multi-tone measurement system with the capability of broadband active baseband (IF) and RF load-pull

This paper utilizes a broadband active load-pull architecture, to overcome these limitations. It incorporates a "open loop" architecture not at RF but at the baseband frequency (IF) to ensure that the injected signal is a modified version (direct function) of the DUT output signal, hence maintaining the required constant emulated load impedance as drive level changes, across the modulation bandwidth. Measurements presented in [8-10] have shown the architecture to be stable. The immediate advantage of the system is the increased speed of device characterization, achieved by removing the iterative nature of setting the load. As this system is drive level independent, the load does not have to be set for each change of the input stimulus making measurements such as power sweeps many, many times faster than the measurement system used in [11-12]. More excitingly the system opens up the opportunity to bring active load-pull into the multi-tone domain, opening up a number of novel applications for the system.

II. MULTI-TONE SIGNALS SAMPLING ISSUES

Triggering has long been an issue surrounding sampling oscilloscopes. It requires the user to provide an external trigger signal to enable measurements, thus adding complexity to the design of such systems. The sampling method discussed in this section overcomes this problem using an internal clock signal in the oscilloscope to trigger waveforms. From this internal clock signal a sub-sampling frequency is determined; the desired carrier frequency is then tweaked to line up with this natural sub-sampling frequency of the oscilloscope.

Furthermore to measure multi-tone signals there are various problems to consider the first is the sheer volume of data that must be collected. This is because the measurement grid is defined by the modulation frequency. The modulation frequency tends to be orders of magnitude smaller than the carrier signal; many data points must be collected to measure the waveform. To overcome this issue the sampling is arranged in such ways that if the collected waveform is transformed to the frequency domain then all locations contain relevant information.

The following equations allow the user to select a desired carrier frequency, modulation frequency and order. The equations are then used to create a new carrier and modulation frequency which lie on the sampled grid, arranged in such a way to completely fill the spectrum in the frequency domain. The sampling method is defined by the steps outlined below. In order to correctly sample the carrier, it must be some multiple of the sub-sampling frequency (sub_freq), it can be seen that the closest multiple M is given by the

following equation (1), where M is rounded to the nearest integer.

$$M = Req_Carrier_Freq / Sub_Freq \quad (1)$$

Given that the Tektronix Sampling Oscilloscope can only measure a set number of points in any sampling window, it can be seen that all measured frequencies must be on a δF grid which given by equation (2).

$$\delta F = (1/Points) * Sub_Freq \quad (2)$$

As we are measuring a modulated waveform we need to sample tones and inter-modulation products around the carrier. To allow this we must move the Location of the carrier in the Frequency grid. If order is the desired number of frequency locations either side of the carrier, then it is clear that the desired location of the carrier in the grid is given by the following equation (3).

$$Location = 2 * Order + 1 \quad (3)$$

It can therefore be seen that the required Carrier frequency (Fcarrier) is given by equation (4).

$$Fcarrier = (M * Sub_Freq) + (Location * \delta F) \quad (4)$$

Substituting for δF from equation (2) and re-arranging gives equation (6)

$$Fcarrier = (M + \frac{Location}{Points}) * (Sub_Freq) \quad (5)$$

To efficiently use the spectrum we require that Fcarrier-Fmod (the lower tone) is on the same grid but at (location -1). Again we must find the closest multiple of the sub-sampling frequency. If X is the closest multiple of the sub-sampling frequency to the required modulation frequency then X is computed using equation (6).

$$X = Round(Req_Mod_Freq / Sub_Freq) \quad (6)$$

Then it can be seen that the closest multiple of sub_freq to (Fcarrier-Fmod), N must be given by the following equation (7).

$$N = M - X \quad (7)$$

The following equation (8) can then be used to find new modulation frequency (Fmod).

$$Fcarrier - F\,mod = N * Fsub + ((Location - 1) * \delta F \quad (8)$$

Substituting for Fcarrier, N and δF from equations (2), (3) and (5) respectively, gives the following equation (9) for Fmod.

$$F\,mod = \left(X + \frac{1}{Points} \right) * Fsub \quad (9)$$

What we end up with in the frequency domain is a number of sections each containing all relevant data related to that particular harmonic of the carrier frequency as shown in the diagram in figure 2, where a waveform with order of 4 is illustrated.

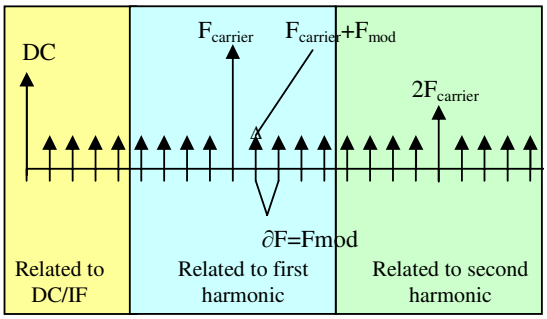

Fig. 2. Representation of sampled spectrum in the frequency domain

It can be seen that multi-tone waveforms can now be sampled efficiently; however there is a further problem to consider. The problem is caused by the fact that there is a minimum hold time between each trigger, defined by the minimum time required to reset the trigger circuitry of the oscilloscope. This means that the envelope and RF signals appear to drift in time but at different rates, making it impossible to trigger the signals to allow for the internal averaging function to be used on the oscilloscope. To overcome this problem, a software triggering function is used to

average the waveforms. The software takes the first waveform collection as a reference data set; all subsequent waveforms are then mathematically realigned to the reference data set to allow for averaging of the waveforms. When multi-tone waveforms are aligned correctly and synchronized with a multi-tone signal source, complex modulated waveforms can be accurately averaged, as depicted in Fig. 3.

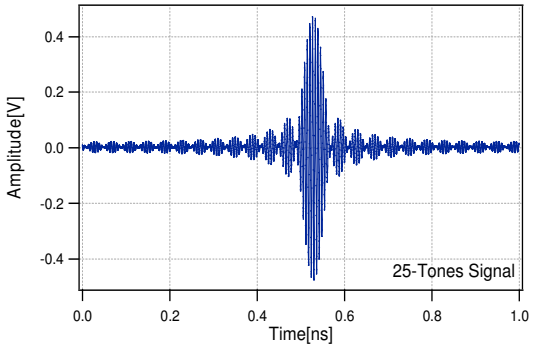

Fig. 3. Complete modulation cycle of on oscilloscope averaged 25-Tones signal at a carrier frequency of 2GHz with 500KHz tone separation.

III. MEMORY EFFECT MEASUREMENTS AND ANALYSIS

To demonstrate the capability of measurement system, baseband load-pull measurements were conducted with RF terminated with nominal 50Ω. The measurements presented here are for CREE CGH40010 discrete 10W GaN HEMT device characterized at centre frequency of 2GHz for 2MHz modulation frequency. The measurements were performed using a fully calibrated measurement system with the device biased at a drain voltage of 28V and a gate voltage of -2.5V resulting in a quiescent current of 250mA. The input stimulus composed of nine equally spaced tones with peak-to-average of 9.54dB, all of equal amplitude but random phases to emulate a real wideband signal [13].

The device delivered 39.5dBm peak envelope power(PEP) when driven approximately 1.5dB into compression and active IF load-pull was used to present the constant baseband impedance to most significant components IF1 (twice the modulation frequency) and IF2 (four times the modulation frequency), the higher baseband components IF3 (six times the modulation frequency) and IF4 (eight times the modulation frequency). Fig. 3 depicts the contours of lower adjacent channel power ratio ($ACPR_L$) when a measurement grid was swept to find the optimum for reduction of memory effects, as it is reported in [13]-[14] that the linearizability of memory-less device is much better than the devices with memory.

The significant observation to note is that there are pronounced ACPR variations and asymmetry around the measurement grid. These measurements suggested that the optimum baseband load for minimum asymmetries is indeed located at point-A and then terminating the baseband components at an experimentally determined optimum point-A, a reduction of approximately 10dB in ACPR was observed in comparison with point-B and it highlights the strong dependence of ACPR on the baseband impedance termination

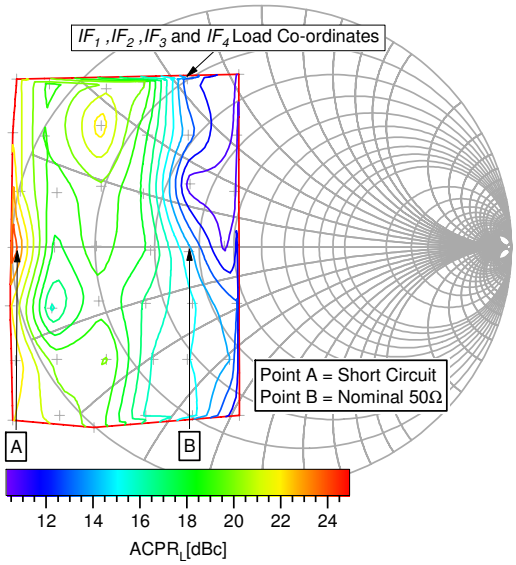

Fig. 3. Baseband load-pull characterization of 10W GaN HEMT under multi-tone stimulus

Fig. 4 shows the output spectra for two cases when different baseband termination is maintained for the baseband components. Terminating the baseband components at point-B

caused a ripple to appear on the DC drain voltage present at the device output plane, which effectively resulted in additional modulation of the RF signal. This, then, lead to the change in the ACPR levels and can be seen there exists a significant memory effects with more than 6dB ACPR asymmetry between upper and lower ACPR products. For the case when optimum impedance is maintained to the baseband components at modulation frequency of 1MHz there are no baseband electrical memory effects, so the spectral regrowth shows no asymmetry for optimum baseband impedance termination. The measured output RF voltage envelopes obtained for the two baseband impedance conditions, are shown in Fig. 5.

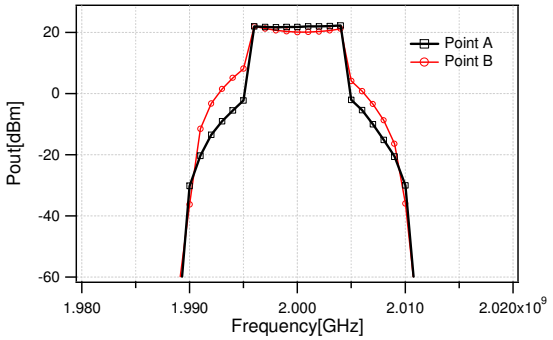

Fig. 4. Measured output spectrum, when different impedances were provided to baseband components with nominal 50Ω RF termination.

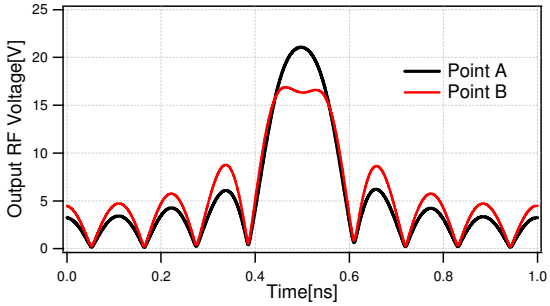

Fig. 5. Measured RF output voltage envelopes for different baseband impedance environment for 2MHz modulation frequency.

In the case of baseband impedance at point-B, an asymmetrical envelope is clearly observed that determines which ACPR product will have the greater magnitude. Whilst terminating the baseband components at point-A, which has been demonstrated to be the optimum load termination, an undistorted output envelope is produced. The broadband baseband short circuit (Γ_{IF} =1∠180°) impedance termination was utilized as shown in Fig. 6, for modulation frequency ranging from 0.5 MHz to 7 MHz, in order to achieve the symmetrical ACPR response. The magnitude of the IF reflection coefficient could not be brought precisely to short for frequency components above 10 MHz due to bandwidth limitation of baseband load-pull PA. For example, the third harmonic of 6 MHz at 18 MHz could not be adequately controlled.

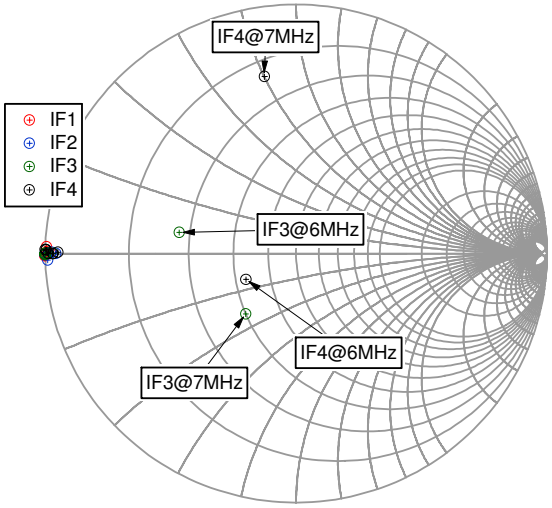

Fig. 6. Measured IF1, IF2, IF3 and IF4 for modulation frequency ranging from 0.5 MHz to 7 MHz.

Fig. 7 shows how the fundamental output power remains constant and independent of the modulation frequency.

With regard to the ACPR distortion $ACPR_L$ and $ACPR_H$, it is clear that the symmetry level of ACPR is degraded at a higher modulation frequency after 5 MHz which is due to impedance variations in higher baseband components (IF3 and IF4), as shown in Fig. 8. It is important to note that the observed variations in $ACPR_L$ and $ACPR_H$ magnitude observed

below 1 MHz are not related to variations in baseband impedance and attributable to other sources of memory, e.g. trapping and thermal effects.

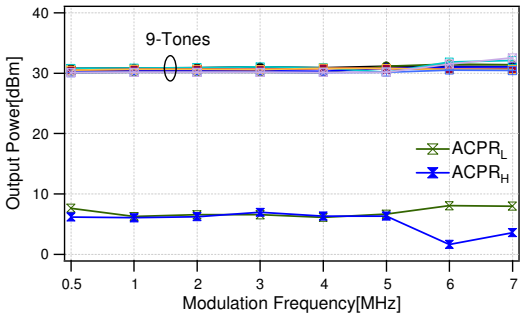

Fig. 7 Measured fundamentals and ACPR power for different modulation frequencies.

IV. COMPREHENSIVE OUT-OF-BAND IMPEDANCE CONTROL

To further demonstrate the broadband load-pull capabilities of the measurement system in engineering the out-of-band impedance environment at RF, a class-J mode was emulated by presenting established impedances [15] at the device package plane. The device was deep class-AB biased, and driven approximately 2dB into compression with a 9-tone modulated excitation centered at 2GHz with a 2MHz tone spacing. Optimum reactive fundamental impedance was presented to all fundamental tones and a suitably phased reactive second harmonic impedance termination was presented to the tones around the 2nd harmonic.

The ability of the system to maintain baseband, fundamental and second harmonic loads is critical over a wider bandwidth. This capability is evident in Fig. 8 where the second harmonic and fundamental loads are kept constant with a slight spreading in the emulated load reflection coefficients takes place. The emulation of desired load reflection coefficients at the baseband causes the spreading to occur at the respective tones around the fundamental and 2nd harmonic impedances. The load emulation around the frequency bands of interest is repetitive process under complex tones (i.e. more than two and three tones), however, every effort was made to minimize the spread to demonstrate the system capability in emulating the impedances when the device was subjected to complex multi-tone excitation. Plotting the measured (RF, IF & DC) time-domain voltage vs. time-domain current yields a complete dynamic load-line which is used to describe the trajectory of the modulated envelope relative to the device's DC characteristic. This intuitive view shows the actual voltage and current behaviour at the calibrated reference plane, and importantly, the nature of any interaction between the envelope and device boundary conditions.

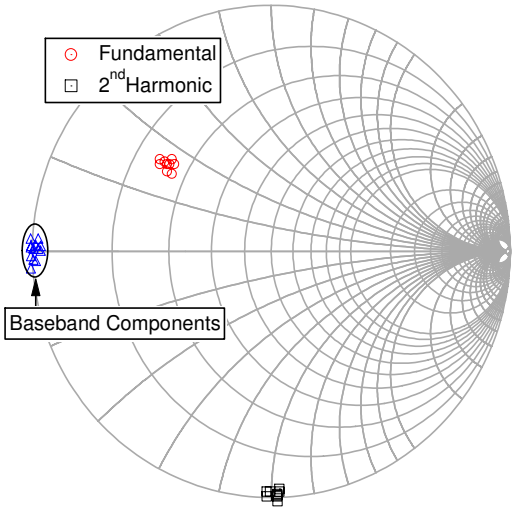

Fig. 8. Measured baseband loads for a class-J emulated RF impedance environment.

Fig.9 shows the dynamic RF and IF load-lines for short circuit baseband impedance. In the case of baseband electrical memory, the IF load-line 'pushes' or 'pulls' the dynamic RF load-line asymmetrically into the knee region of the device.

A Perfect IF short circuit impedance resulted in a straight, vertical IF load-line, and the shape of the IF load-line allows scope for baseband waveform engineering and optimisation for example of the proximity of dynamic RF load-line to knee boundary region. As can be seen from Fig. 9,

IJMOT

INTERNATIONAL JOURNAL OF MICROWAVE AND OPTICAL TECHNOLOGY,

VOL.8, NO.3, MAY 2013

terminating the baseband components with short circuit impedance resulted in static IF voltage, consequently, no variations in $ACPR_L$ and $ACPR_H$ were observed.

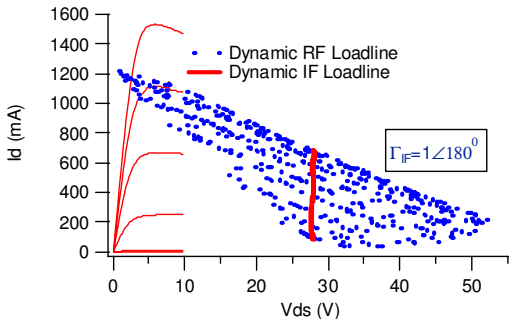

Fig. 9. The measured dynamic RF and IF load-lines for baseband reflection coefficients ($\Gamma_{IF}=1\angle 180^0$)

Fig. 10 shows the measured RF 9-tone power performance as a function of input drive level for 2MHz modulation frequency. The behavior of $ACPR_L$ and $ACPR_H$ is clearly identical when short circuit impedance was presented to all the significant baseband components under class-J mode of operation. It is important and interesting to note that measurement system is effective in presenting constant impedances to baseband components when RF components are terminated with reactive impedances. This highlights the effectiveness of measurement system in engineering comprehensively out-of-band impedance environment.

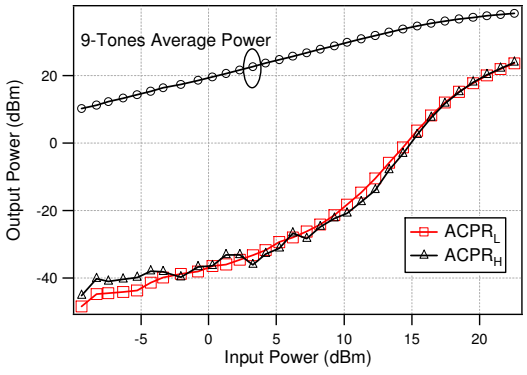

Fig. 10. Measured dynamic power sweep for 9-Tone stimulus for 2MHz modulation frequency.

V. CONCLUSION

This paper has detailed the sampling technique employed to average multi-tone waveforms when integrated with the enhanced waveform measurement system [10] has enabled the measurement and characterization of baseband electrical memory effects under multi-tone stimuli. The 9-tone measurements noticeably showed the effect of the baseband impedance variations on 10 W GaN HEMT ACPR behaviour and induced ACPR asymmetry. The measurement system has been verified and validated through comparison with previous observations using earlier systems; relating to identification of optimal baseband impedances for the reduction of baseband electrical memory effects and linearity [10].

The true benefit of this system becomes apparent through the broadband emulation of a class-J mode of operation under nine-tone stimuli. The results suggest that the suppression of baseband electrical memory has been achieved by simultaneously engineering the most significant IF components and higher order IF components. The results also highlight optimum IF impedance terminations that minimize overall in-band distortion. This important observation then in turn enables an accurate design of PA bias networks.

REFERENCES

[1] R. B. Stancliff and D. P. Poulin, "Harmonic load-pull," *IEEE MTT-S International Microwave Symposium Digest*, 1979, pp. 185 – 187.

[2] D.J. WiILiams, 1. Leckey, P.J. Tasker "A Study of the Effect of Envelope Impedance on intermodulation asymmetry using a two-tone Time Domain Measurement System*" IEEE MTT-S Int. Microwave Symposium*, pp . Dig., Vol. 3, 2002 pp. 1841-1844

[3] A. Alghanim, J. Benedikt, P.J. Tasker, P "A measurement test-set for characterisation of high power LDMOS transistors including memory effects" *Proceedings of High Frequency Postgraduate Student Colloquium*, Page(s):29 – 32, 5-6 September 2005.

[4] A. Alghanim, J. Lees,T. Williams, J. Benedikt, P.J. Tasker, P "Using active IF load-pull to

investigate electrical base-band induced memory effects in high-power LDMOS transistors**,**" *Proceedings of Asia-Pacific Microwave Conference*, Page(s):1 - 4, December 2007.

[5] Maury Microwave "Passive load pull system", www.maurymw.com.

[6] G.P. Bava, U. Pisani, V. Pozzolo, "Active Load Technique for Load-Pull Characterisation at Microwave Frequencies" *IEE Electronic Letters,* 18th February 1982, Vol. 18, No. 4, pp. 178-180.

[7] Yoichiro Takayama "A New load-Pull Characterisation Method for Microwave Power Transistors" *IEEE MTT-S international Microwave Symposium Digest,* 1976, pp. 218-220.

[8] M. Akmal, J. Lees, S. Bensmida, S. Woodington, J. Benedikt, K. Morris, M. Beach, J. McGeehan, P. J. Tasker, " The Impact of Baseband Electrical Memory Effects on the Dynamic Transfer Characteristics of Microwave Power Transistors", in Proc. of *4th International Nonlinear Microwave Monolithic Integrated Circuit(INMMIC)*, pages: 148 – 151, April 2010.

[9] M. Akmal, V. Carrubba, J. Lees, S. Bensmida, S. Woodington, J. Benedikt, K. Morris, M. Beach, J. McGeehan, P. J. Tasker, "Linearity Enhancement of GaN HEMTs under Complex Modulated Excitation by Optimizing the Baseband Impedance Environment", in Proc. of *IEEE MTT-S International. Microwave Symp*osium, page(s):1-4, June 2011.

[10] M. Akmal, J. Lees, S. Bensmida, S. Woodington, V. Carrubba, S. Cripps, J. Benedikt, K. Morris, M. Beach, J. McGeehan, P. J. Tasker, "The Effect of Baseband Impedance Termination on the Linearity of GaN HEMTs", *40th IEEE European Microwave Con*ference(EuMC), pages: 1046 - 1049, September 2010.

[11] A. Alghanim, J. Benedikt, P.J. Tasker, P "A measurement test-set for characterisation of high power LDMOS transistors including memory effects" *Proceedings of High Frequency Postgraduate Student Colloquium*, Page(s):29 – 32, 5-6 September 2005.

[12] A. Alghanim, J. Lees,T. Williams, J. Benedikt, P.J. Tasker, P "Using active IF load-pull to investigate electrical base-band induced memory effects in high-power LDMOS transistors**,**" *Proceedings of Asia-Pacific Microwave Conference*, Page(s):1 - 4, December 2007.

[13] M.Akmal, "An Enhanced Modulated Waveform Measurement System" Ph.D. thesis, Cardiff University, November 2011.

[14] J. P. Martins, P. M. Cabral, N. B. Carvalho,J. C. Pedro, "A Metric for the Quantification of Memory Effects in Power Amplifiers", *IEEE Trans. Microw, Theory and Tech.,* vol. 54, December 2006, pages: 4432-4439.

[15] P. Wright, J. Lees, P. J. Tasker, J. Benedikt, S.C. Cripps, "An efficient, linear, broadband class-J-mode PA realised using RF waveform engineering", *in Proc. of IEEE MTT-S International*, pages: 653 -656, June 2009.]